# Beach morphodynamics in the lee of a wave farm

Javier Abanades[#1], Deborah Greaves[#2], Gregorio Iglesias[#3]

[#]*School of Marine Science and Engineering, Plymouth University*
*Marine Building, Drake Circus, Plymouth, PL48NH (UK)*

[1]javier.abanadestercero@plymouth.ac.uk

[2]deborah.greaves@plymouth.ac.uk

[3]gregorio.iglesias@plymouth.ac.uk

***Abstract*— The significant advances in the past years towards the consolidation of wave energy as a major renewable warrant the investigation of the synergies between this novel resource and coastal defence. The aim of this work is to examine the effects of a wave farm operating at different distances from the coastline on the beach morphology. On the one hand, the impacts of the wave farms on the sediment transport are assessed. On the other hand, how the farm affects the modal state of the beach with reference to a baseline (no farm) scenario is examined. For this purpose, a high-resolution nearshore wave propagation model is coupled to a coastal processes model to assess the wave farm impacts on the beach. The wave farm is found to reduce significantly the erosion in the beach. This is a bonus to be added to the primary role of the wave farm – and one which enhances its economic viability by leading to savings in conventional coastal defence measures.**

***Keywords* — Wave energy, Wave farm, Wave Energy Converter, Nearshore impact, Beach profile, Erosion**

## I. Introduction

A wave farm extracts the energy from the waves through Wave Energy Converters (WECs). This extraction of energy implies a reduction in the incident wave height nearshore, which in turn may modify the patterns of sediment transport and eventually lead to an attenuation of erosion. This paper is concerned with the question as to whether wave farms can be used for coastal protection and in which manner this is influenced by the farm-to-coast distance.

Previous studies focused on the impact of wave farms on the wave conditions [1-10] showed a significant reduction in the wave height in the lee of the wave farm. Abanades, et al. [11] proved that this extraction resulted in a medium-term reduction of the erosion exceeding 20% in some sections of the beach profile (2D). In further studies, Abanades, et al. [12], [13] considered the 3D response of the beach under storm conditions in order to establish the applicability of wave farms to coastal defence. Erosion was found to decrease by more than 50% in certain areas of the beach. In the wake of these studies, which evidenced the impact of wave farms on beach morphology, this paper considers three farm-to-coast distances: 2 km, 4 km and 6 km from the 10 m water depth contour [2], to determine the wave farm impacts on the beach morphology as a function of them.

The objective of this paper is twofold: the analysis of the wave farm impacts on the sediment transport patterns, and the quantification of the modal state of the beach with and without the wave farm during a year. As for the former, the response of the beach is analysed under frequent storm conditions to establish the degree of coastal protection offered by the wave farm as a function of the distance. As for the latter, the percentages of time in an average year corresponding to each beach modal state in the baseline scenario, and how these percentages are altered by a wave farm as a function of its distance from the coast are quantified.

For this purpose, process-based modelling, analytical solutions and empirical classifications are applied in a case study at Perranporth Beach, UK (Fig. 1). To analyse the response of the beach two process-based models are coupled: SWAN [14], a wave propagation model used to represent the wave field-WEC array interaction; and XBeach [15], a coastal processes model to determine the effects of the farm on the beach dynamics. For the case of the beach modal state, the morpohology of the beach is determined by means of an empirical classification that accounts for breaking wave conditions, tidal regime and sediment size. To calculate the breaking wave conditions, the results of the wave propagation model are coupled to the Kamphuis' formulae [16].

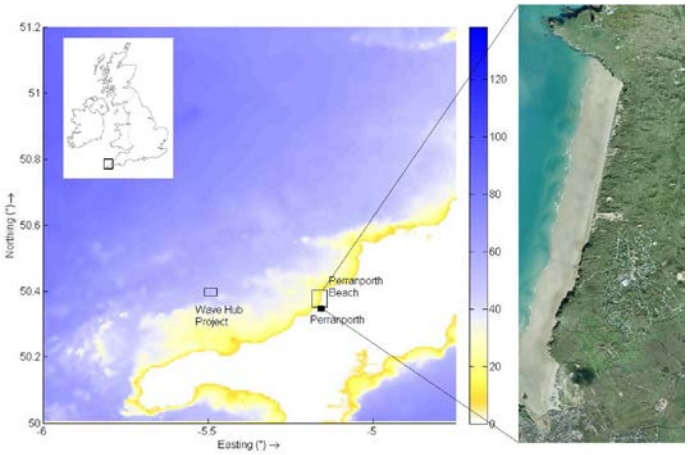


Fig. 1 Bathymetry of SW England [water depths in m] including the location of Perranporth Beach, the WaveHub Project and an aerial photo of Perranporth Beach [source: Coastal Channel Observatory].

## II. Materials and Methods

### A. Case study: Perranporth Beach

For the present paper Perranporth Beach, located in the Cornwall Coast (SouthWest England), was selected as a case

study to analyse the impacts of wave farms. This coast is one of the areas with greatest potential for wave energy since it was selected to house the Wave Hub project — a grid-connected offshore facility for sea tests of WECs. Perranporth Beach is a 3.6 km beach composed of medium quartz sand, $D_{50}$ = 0.27 – 0.29 mm [17] and a relatively flat intertidal area, tan β = 0.015 – 0.025. The bathymetry data obtained through field survey by the Coastal Channel Observatory were used.

Perranporth faces directly toward the North Atlantic Ocean and it has experienced an increase in flooding and erosion risks from rising sea levels and increased storminess [18], as was shown during the energetic storms in 2014. Therefore, Perranporth constitutes a prospective location for using such wave farms for coastal defence. During the year studied to establish the modal state of the beach (November 2007 to October 2008), the average values of the significant wave height ($H_s$), peak period ($T_p$) and direction ($\theta$) were 1.60 m, 10.37 s and 282.59 °, respectively. In the case of the short-term analysis for determining the impacts of wave farms on the sediment transport patterns, two wave conditions representative of the offshore wave climate in the area [19] were chosen (Table 1).

| Case study | $H_s$ (m) | $T_p$ (s) | $\theta$ (°) |
|---|---|---|---|
| CS1 | 3 | 12 | 315 (NW) |
| CS2 | 3.5 | 11 | 315 (NW) |

Table 1: Offshore wave conditions: significant wave height (*Hs*), peak period (*Tp*) and mean direction ($\theta$) for the different case studies.

### *B. Process-based modelling: coupling SWAN-XBeach*

The wave propagation was carried out using SWAN, a third-generation phase-averaged wave model for the simulation of waves in waters of deep, intermediate and shallow depth. SWAN computes the evolution of the wave spectrum based on the spectral wave action balance equation.

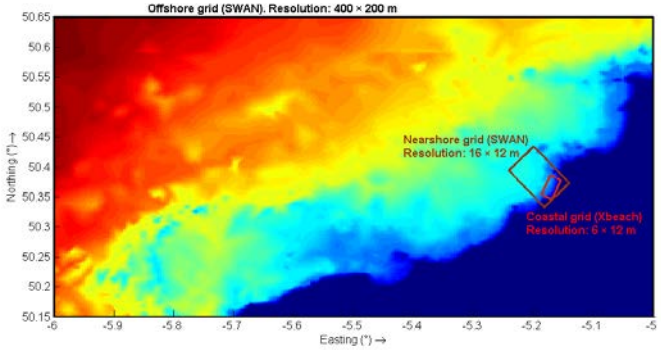


Fig. 2: Computational grids of the wave propagation and the coastal processes model

A high-resolution grid was essential in this work in order to: (i) implement the WECs that formed the wave farm in their exact position, (ii) represent accurately the impact of the wave farm on the wave conditions in its lee, and (iii) couple the results to the coastal processes model and the Kamphuis' formulae. On this basis, two computational grids are defined (Fig. 2): (i) an offshore grid covering approx. 100 km × 50 km with a grid size of 400 × 200 m, and (ii) a high-resolution nearshore (nested) grid covering the study area, with dimensions of approx. 8 km × 6 km and a grid size of 16 m × 12 m.

The wave farm consisted of 11 WaveCat WECs arranged in two rows, with a spacing between devices equal to 2.2D, where $D$ = 90 m is the distance between the twin bows of a single WaveCat WEC and corresponds to the capture width of the device. The farm was located at distances of 2 km, 4 km, and 6 km (Fig. 3) from a reference contour (10 m water depth), which corresponded to water depths of approx. 25 m, 30 m and 35 m, respectively [2, 10]. The WEC-wave field interaction was modelled by means of the results obtained for the wave transmission coefficient in the lee of the device in the laboratory tests carried out by Fernandez, et al. [20].

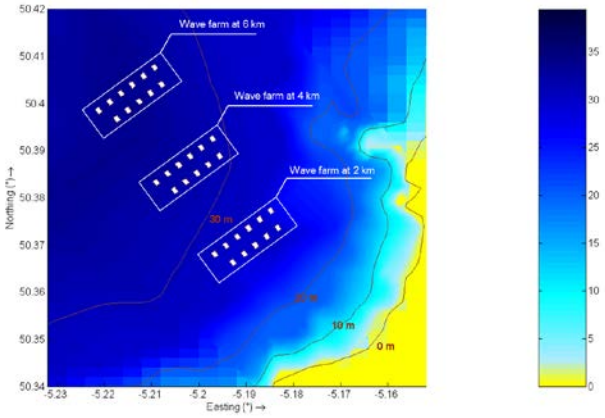


Fig. 3: Wave farm located at different distances: 2 km, 4 km and 6 km to the 10 m water depth contour at Perranporth Beach [water depth in m].

Based on the results of the wave propagation model, the coastal processes model, XBeach, was used to compute the impact of the wave farm on beach morphology. XBeach is a 2DH (two-dimensional horizontal) time-dependent model that solves coupled cross-shore and alongshore equations for wave propagation, flow, sediment transport and bottom changes. The full description of the model can be found in Roelvink, et al. [15].

XBeach has been widely validated to determine the impact of storms on sandy [21-23] and gravel beaches [24-27] at different locations. In this case, the impact of the wave farm on the beach morphology (3D) was compared to the baseline scenario at Perranporth Beach following the model set up applied by Abanades, et al. [11] at the same location. The high-resolution grid implemented on XBeach covered an area of 1.4 km cross-shore and 3.0 km alongshore at Perranporth Beach with a resolution of 6 m and 12.5 m, respectively. The bathymetry data, from the Coastal Channel Observatory, were interpolated onto this grid (Fig. 4), which comprised elevation values from -20 m to more than 60 m with reference to the local chart datum (LCD). The maximum values correspond to the top of the dune, which backs most part of the beach (from Profile P3 in Fig. 4 to the northernmost point of the beach), and it is characterised by a very steep section (from Profile P3

to Profile P2) that will be of relevance in the beach morphodynamics.

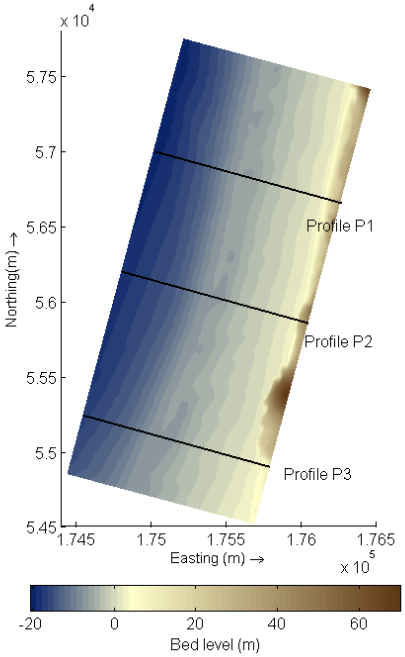


Fig. 4: Bathymetry of Perranporth Beach computed in XBeach. Profiles P1, P2 and P3 included. Water depth in relation to local chart datum [in m].

The effects of the wave farm on the beach were determined based on a comparison of the different wave farm scenarios with the baseline (no farm) case. The impact indicators defined by Abanades, et al. [12] are considered:

- Bed Level Impact (*BLI*) that represents the sea bed level difference between the baseline and the wave farm scenario at a generic point of the beach. A positive value signifies that the seabed level is higher in the presence of the wave farm, and, therefore a reduction of the erosion in that point.
- Beach Face Eroded Area ($FEA_b$ or $FEA_f$) that quantifies the erosion in the beach face (area over the mean water level exposed to the action of the waves) in the baseline and the wave farm scenario. A negative value means an accretion in this area.
- Non-dimensional Erosion Reduction (*NER*) that computes the variation in the eroded area as a fraction of the total eroded area brought about by the wave farm. A positive or negative value implies a reduction or increase in the eroded area, respectively, as a result of the wave farm.

### *C. Beach modal state*

The conceptual beach classifications are empirical models based on the relationships between the characteristics of different types of beaches (wave climate, sediment size and tidal regime) and field observations. Therefore, these models allow the evolution of beach dynamics as a function of the beach features to be predicted, and also, the quantification of the potential changes induced by a modification of these, such as the reduction of wave energy brought about by a wave farm.

The empirical classification presented by Masselink and Short [28], based on the classification of Wright and Short [29], depends on two parametes: the dimensionless fall velocity parameter, ($\Omega$), also known as Dean's number [30] and the Relative Tide Range (*RTR*), defined as

$$\Omega = \frac{H_b}{w_s T} \tag{1}$$

$$RTR = \frac{MSR}{H_b} \tag{2}$$

where $H_b$ is the breaking wave height, $T$ is the wave peak period corresponding to the breaking conditions, $w_s$ is the sediment fall velocity and *MSR* the Mean Spring tidal Range (*MSR* = 6.3 m at Perranporth).

Fig. 5 shows the relationships between the dimensionless fall velocity and the relative tide range parameters that are used to establish the modal beach state. As the RTR parameter increases the beach evolves from a classic reflective state through the formation of a low tide terrace at the toe of the beach face and low tide rips to a steep beach face fronted by a dissipative low tide terrace. In the case of an intermediate barred beach, the increase in the tidal range moves the bar down to the low tide level generating a low tide bar and rips. Finally, for barred dissipative beaches characterised by multiple subdued bars at different water depths, the increase of RTR results in the disappearance of these bars. The latter two groups shift to ultra-dissipative beaches with values of RTR between 7-15. For values of RTR greater than 15 the resulting beach is fully tide-dominated.

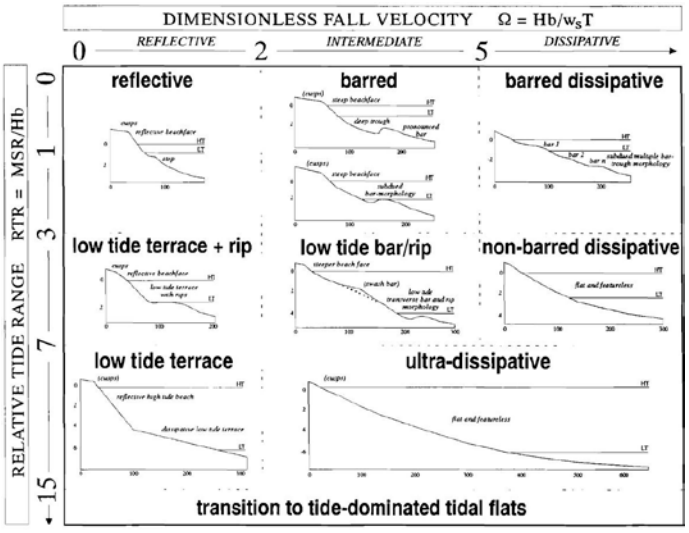


Figure 5: Conceptual beach model [28].

To determine the wave conditions necessary to establish the morphological beach state – breaking wave height ($H_b$) and peak period ($T_p$) the results from SWAN are coupled to the

Kamphuis' formulae [16], a breaking criterion for irregular waves based on the following expressions:

$$H_{sb} = 0.095 e^{4m} L_{bp} \tanh\left(\frac{2\Pi d_b}{L_{bp}}\right) \quad \text{, and} \quad (3)$$

$$\frac{H_{sb}}{d_b} = 0.56 e^{3.5m} \quad , \quad (4)$$

where $H_{sb}$ represents the breaking significant wave height, $m$ the beach slope, $L_{bp}$ the breaking wave length and $d_b$ the breaking water depth. Once he breaking wave height was determined, the corresponding period was selected.

## III. Results and Discussion

The wave propagation model was validated using the wave buoy data at Perranporth Beach from November 2007 to October 2008, missing out January 2008 owing to the lack of data. Fig. 6 shows the good fit achieved between the significant wave height computed by SWAN and the values from the wave buoy. The coefficient of determination, $R^2$, and the Root Mean Square Error, *RMSE*, confirm the goodness of the fit: $R^2 = 0.94$ and *RMSE* = 0.38 m.

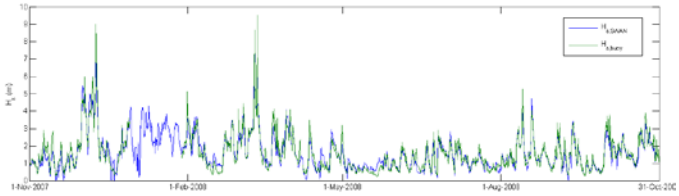

Figure 6: Time series of simulated (*Hs, SWAN*) and measured (*Hs, buoy*) significant wave height.

In first place, the wave farm impacts on sediment transport are analysed. The nearshore significant wave height ($H_s$) for the different scenarios (baseline and with the wave farm at distances of 2 km, 4 km and 6 km from the reference contour) is shown in Figure 7 for CS1 (Table 1). The reduction in the significant wave height in the lee of the farm caused by the energy extraction is apparent. The maximum values of the reduction were achieved in all the wave farm scenarios behind the second row of WECs with values of up to 50%. At a distance of 1.5 km from the second row of devices, the reduction reached a peak of 40% due to the merging of the shadows caused by the first and the second row of devices. However, this reduction decreased moving towards the coast due to the redistribution of the energy from the edges into the shadow caused by the wave farm. At a water depth of 10 m in the area of Perranporth Beach, the average reduction along this contour in the area of caused by the wave farm closest to the coast (2 km) was approx. 25%, whereas for the wave farm at 4 and 6 km the average reduction was approx. 15% and 9%, respectively.

The relevance of the farm-to-coast distance may be readily observed in the shadows caused by the wave farm at different distances. The area affected at the coastline by the wave farm furthest to the coast (6 km) was greater than 7 km, however the average reduction of the significant wave height in this area was less than 5%. On the other hand, the wave farm at 2 km affected a smaller area in the coastline, around 4 km, but the reduction exceeded 10%.

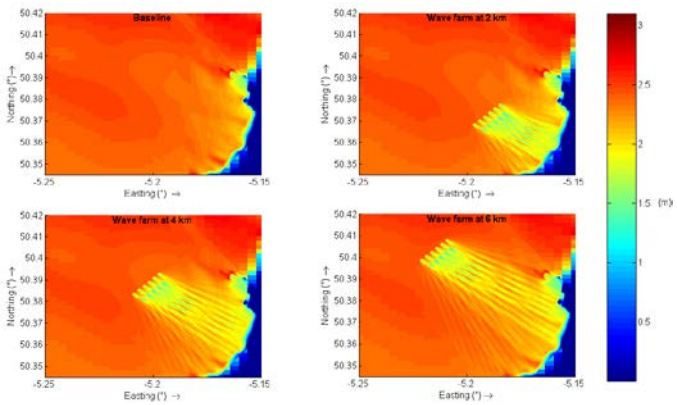


Figure 7: Significant wave height [m] in the baseline scenario and in the presence of the farm at distances of 2 km, 4 km and 6 km from the reference (10 m water depth) contour in CS1 (clockwise from above left).

The results along the 20 m water depth contour (Figure 7) are the input of the coastal processes model to study in which manner the modification of the wave patterns affected the coastal processes and, consequently, the beach morphology. To quantify this alteration the results were analysed by means of the impact indicators defined in Section 3.2. The first indicator was the bed level difference, *BLI*, which represented the difference of the bed level between the baseline and the wave farm scenarios at a point in time. Figure 8 shows *BLI* values at the end of the storm for CS1 with the wave farm at a distance of 2 km (left), 4 km (middle) and 6 km (right). It was observed that the main impact caused by the wave farm was located at the beach face, where reductions of the erosion up to 1.5 m were found. In the comparison between scenarios, the wave farm at a distance of 2 km caused greater reduction of the erosion in the beach than the other scenarios, in which areas with significant reductions of erosion were combined with negligible values or even accretion.

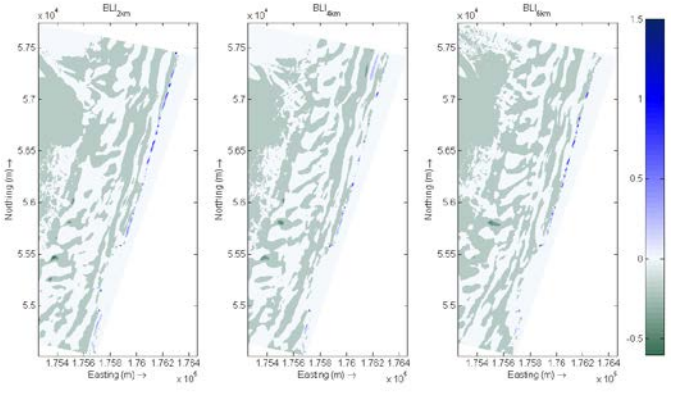


Figure 8: Bed level impact in the area of interest with the wave farm at a distance of 2 km ($BLI_{2km}$), 4 km ($BLI_{4km}$) and 6 km ($BLI_{6km}$) at the end of the storm in CS1.

The impacts on the beach face were analysed through the *FEA* and *NER* indicators. The *FEA* factor was defined to

quantify the erosion in the beach face along the beach (Fig. 9). The greatest values of this indicator along the beach were focussed in the southern area because this section was not backed by the dune. The erosion in the baseline scenario was, in general, greater than the scenarios with the wave farm, especially in the middle and northern area of the beach, *y*–coordinate (along the beach) > 1250 m. To compare the reduction between the different wave farm scenarios the indicator *NER* was defined, which showed the variation of the erosion in terms of the eroded area in the baseline scenario (Figure 10). The *NER* values fluctuated considerably along the beach, but it was observed that the reduction using a wave farm at a distance of 2 km was greater than the other two scenarios.

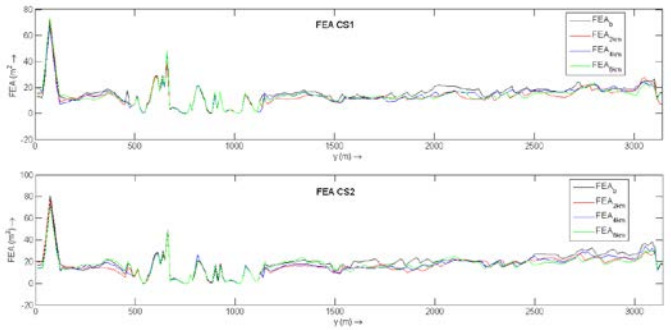


Figure 9: Beach face eroded area in the following scenarios: baseline ($FEA_b$) and with the wave farm at a distance of 2 km ($FEA_{2km}$), 4 km ($FEA_{4km}$) and 6 km ($FEA_{6km}$) along Perranporth Beach (*y* - coordinate, with *y* increasing towards the north of the beach) at the end of the storm in CS1 (above) and CS2 (below).

In the area of the steep dune (500 m < *y*–coordinate < 1250 m), the erosion in the beach face was very low (negligible in some sections), and very few profiles presented an isolated response taking the *NER* factor negative values (greater erosion with the farm than without it). However, in terms of the average reduction of the beach face erosion along the whole beach, it was confirmed that the wave farm at 2 km offered a greater degree of coastal protection, around 15% in both case studies, than the scenario with the wave farm at 4 and 6 km, which presented an approximate reduction of approx. 10%. Considering particular sections of the beach, the impact was much more significant, for instance, the reduction exceeded 20% for the wave farm at 2 km for values of the *y* – coordinate between 1200 and 2000 m in CS2, which was the area most affected by the reduction of the significant wave height (Figure 7).

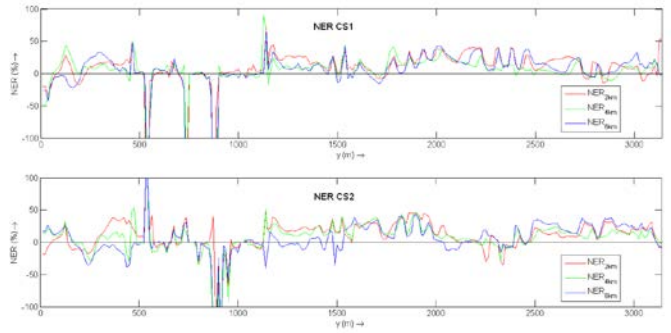


Figure 11: Non-dimensional erosion reduction (*NER*) at the beach face in the following scenarios: with the wave farm at a distance of 2 km ($NER_{2km}$), 4 km ($NER_{4km}$) and 6 km ($NER_{6km}$) along Perranporth Beach (*y*-coordinate, with *y* increasing towards the north of the beach) at the end of the storm in CS1 (above) and CS2 (below).

In second place, the modal state of the beach was determined based on the results of the wave propagation model. In order to investigate the spatial variability of the impact three profiles (Fig. 4) were selected: profiles P1, P2 and P3 corresponded with the south, middle and north section of the beach.

| **Profile P1: South section** | | | | | |
|---|---|---|---|---|---|
| Reflective | | Barred | | Barred dissipative | |
| Baseline | 0.00% | Baseline | 0.07% | Baseline | 16.04% |
| 6 km | 0.00% | 6 km | 0.07% | 6 km | 15.96% |
| 4 km | 0.00% | 4 km | 0.07% | 4 km | 15.90% |
| 2 km | 0.00% | 2 km | 0.07% | 2 km | 15.70% |
| Low tide Terrace + rip | | Low tide bar/rip | | Non-barred dissipative | |
| Baseline | 0.00% | Baseline | 25.50% | Baseline | 26.59% |
| 6 km | 0.00% | 6 km | 25.70% | 6 km | 26.39% |
| 4 km | 0.00% | 4 km | 25.98% | 4 km | 26.18% |
| 2 km | 0.00% | 2 km | 26.18% | 2 km | 25.77% |
| Low tide terrace | | Ultra-dissipative | | | |
| Baseline | 3.36% | Baseline | 22.89% | | |
| 6 km | 3.36% | 6 km | 22.89% | | |
| 4 km | 3.43% | 4 km | 22.82% | | |
| 2 km | 3.36% | 2 km | 23.24% | | |
| Transition to tide-dominated tidal flat | | | | | |
| Baseline | 5.55% | | | | |
| 6 km | 5.63% | | | | |
| 4 km | 5.62% | | | | |
| 2 km | 5.69% | | | | |

Table 2: Percentages of the beach modal state for the south section of the beach (Profile P1) from 1st November 2007 to 31st October 2008

The south section of the beach is predominantly dissipative (third column in the table), although the percentage that the beach is found to be intermediate (second column) is far from negligible. Indeed, in the case with the farm at a distance of 2 km, the low tide bar/rip becomes the most frequent state. The comparison between the baseline and farm scenarios reflects a slight modification of the modal state of the beach owing to the low impact of the wave farm on the wave conditions in this area. The maximum difference between the baseline and the farm scenarios is the case of the non-barred dissipative state, in which the reduction does not exceed 1%. In any case, the trends due to the reduction of the significant wave height are shown in the results; for instance, the percentage of low tide bar/rip state increases as the wave farm become closer,

because the Relative Range Tidal parameter (RTR) is inversely proportional to the breaking wave height. On the other hand, the dimensionless fall velocity parameter (Ω) is directly proportional to the breaking wave height, and, therefore the barred dissipative state occurred more frequently in the baseline scenario than in the cases with the farm.

| **Profile P2: Middle section** | | | | | |
|---|---|---|---|---|---|
| Reflective | | Barred | | Barred dissipative | |
| Baseline | 0.00% | Baseline | 0.14% | Baseline | 16.59% |
| 6 km | 0.00% | 6 km | 0.07% | 6 km | 15.49% |
| 4 km | 0.00% | 4 km | 0.07% | 4 km | 14.39% |
| 2 km | 0.00% | 2 km | 0.07% | 2 km | 6.18% |
| Low tide Terrace + rip | | Low tide bar/rip | | Non-barred dissipative | |
| Baseline | 0.00% | Baseline | 28.10% | Baseline | 28.71% |
| 6 km | 0.00% | 6 km | 27.55% | 6 km | 28.92% |
| 4 km | 0.00% | 4 km | 28.24% | 4 km | 28.71% |
| 2 km | 0.00% | 2 km | 31.11% | 2 km | 22.62% |
| Low tide terrace | | Ultra-dissipative | | | |
| Baseline | 0.89% | Baseline | 22.68% | | |
| 6 km | 0.96% | 6 km | 23.99% | | |
| 4 km | 1.03% | 4 km | 24.40% | | |
| 2 km | 3.49% | 2 km | 32.28% | | |
| Transition to tide-dominated tidal flat | | | | | |
| Baseline | | 2.89% | | | |
| 6 km | | 3.02% | | | |
| 4 km | | 3.16% | | | |
| 2 km | | 4.25% | | | |

Table 3: Percentages of the beach modal state for the middle section of the beach (Profile P2) from 1st November 2007 to 31st October 2008

In the case of the middle of the beach (Table 3), the results were slightly different compared with the south section. In this area, the wave farm impacts are greater compared to the south section. Whereas the wave farm at 4 km and 6 km do not present significant differences compared with the baseline scenario, the wave farm at 2 km changes the behaviour of the beach significantly, reducing the barred dissipative state by more than 5% or 20 days per year, and increasing the ultradissipative state by more than 15 days. Overall, with the wave farm at 2 km the most frequent state shifted from non-barred dissipative (baseline) to ultra-dissipative due to the reduction of breaking wave height.

Finally, the north section of the beach is the area that presented the greatest differences between the baseline and the farm scenarios (Table 4). The trends mentioned in previous paragraphs are accentuated in this area, the reduction in the barred and non-barred dissipative states results in a greater occurrence of the ultra-dissipative beach, from 5 days to 36 days per year in the case of the farm at 6 and 2 km, respectively – a very substantial change in the morphological behaviour of the beach. As regards the $\Omega$ parameter, it is observed that the closest wave farm make the low tide terrace and the low tide bar and rip states more frequent by 10 and 12 days per year, respectively, compared with the baseline scenario.

| **Profile P3: North section** | | | | | |
|---|---|---|---|---|---|
| Reflective | | Barred | | Barred dissipative | |
| Baseline | 0.00% | Baseline | 0.07% | Baseline | 21.73% |
| 6 km | 0.00% | 6 km | 0.07% | 6 km | 20.90% |
| 4 km | 0.00% | 4 km | 0.07% | 4 km | 20.29% |
| 2 km | 0.00% | 2 km | 0.00% | 2 km | 16.04% |
| Low tide Terrace + rip | | Low tide bar/rip | | Non-barred dissipative | |
| Baseline | 0.00% | Baseline | 22.76% | Baseline | 26.11% |
| 6 km | 0.00% | 6 km | 22.69% | 6 km | 25.63% |
| 4 km | 0.00% | 4 km | 22.62% | 4 km | 25.29% |
| 2 km | 0.07% | 2 km | 23.85% | 2 km | 25.29% |
| Low tide terrace | | Ultra-dissipative | | | |
| Baseline | 2.06% | Baseline | 22.69% | | |
| 6 km | 2.19% | 6 km | 23.85% | | |
| 4 km | 2.19% | 4 km | 24.81% | | |
| 2 km | 3.29% | 2 km | 26.32% | | |
| Transition to tide-dominated tidal flat | | | | | |
| Baseline | | 4.59% | | | |
| 6 km | | 4.66% | | | |
| 4 km | | 4.73% | | | |
| 2 km | | 5.14% | | | |

Table 4: Percentages of the beach modal state for the north section of the beach (Profile P3) from 1st November 2007 to 31st October 2008

In summary, the presence of the wave farm affects the modal state of the beach drastically, decreasing the occurrence of wave-dominated states (barred and non-barred dissipative states) in the favour of tide-dominated (low tide bar and rip in winter and ultra-dissipative in summer). The reduction of the wave-dominated states would seem to lead to an increase in the onshore sediment transport and the removal of the offshore bar, the materials of which would cause accretion on the beach – in line with the findings by Abanades, et al. [11], [12].

## IV. Conclusions

In view of the accelerated pace of development of wave energy, a thorough understanding of the effects of nearshore wave farms on beach morphodynamics will soon be fundamental to coastal management. In this context, this paper

analyses the role played by the farm-to-coast distance to protect the coast.

It was observed that the closer the farm to the coast, the lesser wave energy resource but the greater the reduction of the erosion. The overall reduction of the erosion on the beach face compared to the baseline scenario was 15% for the closest wave farm and approx. 10% for the other two. These values fluctuated significantly along the beach, and in some sections, especially in the northern area of the beach, exceeded 40%.

In the analysis of the beach modal state, it was observed that the wave farm can transform the predominant character of the beach from wave- to tide-dominant. The reduction in the occurrence of the barred states corresponds to an increase of the onshore sediment transport and the removal of the offshore bar, which would in turn lead to accretion of the beach.

In sum, this work showed that a wave farm can alter the behaviour of a beach in its lee considerably. This in itself need not be regarded as a negative impact; on the contrary, the wave farm can lead to beach accretion and thus serve to counter erosional trends. Moreover, the effects of the wave farm on the beach can be controlled by locating the farm closer to, or further from, the shoreline.

## ACKNOWLEDGMENT

This research was carried out in the framework of the Atlantic Power Cluster Project, funded by the Atlantic Arc Programme of the European Commission (2011-1/151) and the School of Marine Sciences and Engineering of Plymouth University. The authors are grateful to the Coastal Channel Observatory and DIGIMAP for providing the data.

## REFERENCES

[1] Beels, C., et al., Numerical implementation and sensitivity analysis of a wave energy converter in a time-dependent mild-slope equation model. Coastal Engineering, 2010. 57(5): p. 471-492.

[2] Iglesias, G. and R. Carballo, Wave farm impact: The role of farm-to-coast distance. Renewable Energy, 2014. 69(0): p. 375-385.

[3] Vidal, C., et al., Impact of Santoña WEC installation on the littoral processes. Proceedings of the 7th European wave and tidal energy conference, Porto, Portugal, 2007.

[4] Smith, H.C.M., C. Pearce, and D.L. Millar, Further analysis of change in nearshore wave climate due to an offshore wave farm: An enhanced case study for the Wave Hub site. Renewable Energy, 2012. 40(1): p. 51-64.

[5] Millar, D.L., H.C.M. Smith, and D.E. Reeve, Modelling analysis of the sensitivity of shoreline change to a wave farm. Ocean Engineering, 2007. 34(5-6): p. 884-901.

[6] Palha, A., et al., The impact of wave energy farms in the shoreline wave climate: Portuguese pilot zone case study using Pelamis energy wave devices. Renewable Energy, 2010. 35(1): p. 62-77.

[7] Zanuttigh, B. and E. Angelelli, Experimental investigation of floating wave energy converters for coastal protection purpose. Coastal Engineering, 2013. 80: p. 148-159.

[8] Ruol, P., et al., Near-shore floating wave energy converters: applications for coastal protection, in Proceedings of the international conference of Coastal Engineering 20102011: Shanghai.

[9] Mendoza, E., et al., Beach response to wave energy converter farms acting as coastal defence. Coastal Engineering, 2014. 87(0): p. 97-111.

[10] Carballo, R. and G. Iglesias, Wave farm impact based on realistic wave-WEC interaction. Energy, 2013. 51: p. 216-229.

[11] Abanades, J., D. Greaves, and G. Iglesias, Wave farm impact on the beach profile: A case study. Coastal Engineering, 2014. 86(0): p. 36-44.

[12] Abanades, J., D. Greaves, and G. Iglesias, Coastal defence through wave farms. Coastal Engineering, 2014. 91(0): p. 299-307.

[13] Abanades, J., D. Greaves, and G. Iglesias, Coastal defence using wave farms: The role of farm-to-coast distance. Renewable Energy, 2015. 75(0): p. 572-582.

[14] Booij, N., R.C. Ris, and L.H. Holthuijsen, A third-generation wave model for coastal regions: 1. Model description and validation. Journal of Geophysical Research: Oceans, 1999. 104(C4): p. 7649-7666.

[15] Roelvink, J., et al., XBeach model description and manual, 2006, UNESCO-IHE Institute for Water Education.

[16] Kamphuis, J., Wave transformation. Coastal Engineering, 1991. 5(3): p. 173-184.

[17] Austin, M., et al., Temporal observations of rip current circulation on a macro-tidal beach. Continental Shelf Research, 2010. 30(9): p. 1149-1165.

[18] CISCAG, Shoreline Management Plan 2011, Cornwall and Isles of Scilly Coastal Advisory Group.

[19] Kenney, J., SW Wave Hub metocean design basis. SWRDA.[Online] Available at, 2009.

[20] Fernandez, H., et al., The new wave energy converter WaveCat: Concept and laboratory tests. Marine Structures, 2012. 29(1): p. 58-70.

[21] Roelvink, D., et al., Modelling storm impacts on beaches, dunes and barrier islands. Coastal Engineering, 2009. 56(11–12): p. 1133-1152.

[22] McCall, R.T., et al., Two-dimensional time dependent hurricane overwash and erosion modeling at Santa Rosa Island. Coastal Engineering, 2010. 57(7): p. 668-683.

[23] Pender, D. and H. Karunarathna, A statistical-process based approach for modelling beach profile variability. Coastal Engineering, 2013. 81(0): p. 19-29.

[24] Williams, J.J., et al., Modelling gravel barrier profile response to combined waves and tides using XBeach: Laboratory and field results. Coastal Engineering, 2012. 63(0): p. 62-80.

[25] McCall, R.T., et al., MODELLING OVERWASH AND INFILTRATION ON GRAVEL BARRIERS. 2012. 2012.

[26] McCall, R., et al., Predicting overwash on gravel barriers. 2013.

[27] Jamal, M.H., D.J. Simmonds, and V. Magar, Modelling gravel beach dynamics with XBeach. Coastal Engineering, 2014. 89(0): p. 20-29.

[28] Masselink, G. and A.D. Short, The effect of tide range on beach morphodynamics and morphology: a conceptual beach model. Journal of Coastal Research, 1993: p. 785-800.

[29] Wright, L. and A.D. Short, Morphodynamic variability of surf zones and beaches: a synthesis. Marine Geology, 1984. 56(1): p. 93-118.

[30] Dean, R.G. Heuristic models of sand transport in the surf zone. in First Australian Conference on Coastal Engineering, 1973: Engineering Dynamics of the Coastal Zone. 1973. Institution of Engineers, Australia.